Room Temperature Hydrogenation of CO2 Utilizing a Cooperative Phosphorus Pyridone-Based Iridium Complex

SIANGWATA, Shepherd, HAMILTON, Alexander, TIZZARD, Graham John, COLES, Simon J. and OWEN, Gareth Richard

ChemCatChem

Supporting Information

Room Temperature Hydrogenation of CO_2 Utilizing a Cooperative Phosphorus Pyridone-Based Iridium Complex

Shepherd Siangwata, Alex Hamilton, Graham J. Tizzard, Simon J. Coles, and Gareth R. Owen*

Supplementary Information for:

Room Temperature Hydrogenation of CO_2 Utilizing a Cooperative Phosphorus Pyridone-Based Iridium Complex

Shepherd Siangwata,[a] Alex Hamilton,[b] Graham J. Tizzard,[c] Simon J. Coles,[c] Gareth R. Owen,[a]*

*[a] Chemical and Environmental Sciences, Sustainable Environment Research Centre (SERC), University of South Wales, CF37 4AT, UK; [b]Sheffield Hallam University, Biomolecular Sciences Research Centre (BMRC) and Department of Biosciences and Chemistry, , Sheffield, UK; [c] National Crystallography Service, University of Southampton, Highfield, Southampton. SO17 1BJ, UK - * Corresponding author. E-mail address: gareth.owen@southwales.ac.uk*

Table of Contents

1. General Remarks

Nuclear Magnetic Resonance (NMR) spectra were recorded on a Bruker 400 MHz Ascend 400 (^{1}H: 400.13 MHz; ^{13}C{^{1}H}: 100.62 MHz, ^{31}P{^{1}H}: 161.97 MHz) spectrometer. NMR chemical shifts were reported relative to the internal standard tetramethylsilane (δ 0.00). FT-IR spectra were recorded using a PerkinElmer Spectrum Two Attenuated Total Reflectance Infrared spectrometer. The mass spectra were collected at Cardiff University. Elemental analysis was carried out at London Metropolitan University.

2. Synthesis and Characterisation of 2-*t*butyloxy-6-bromopyridine

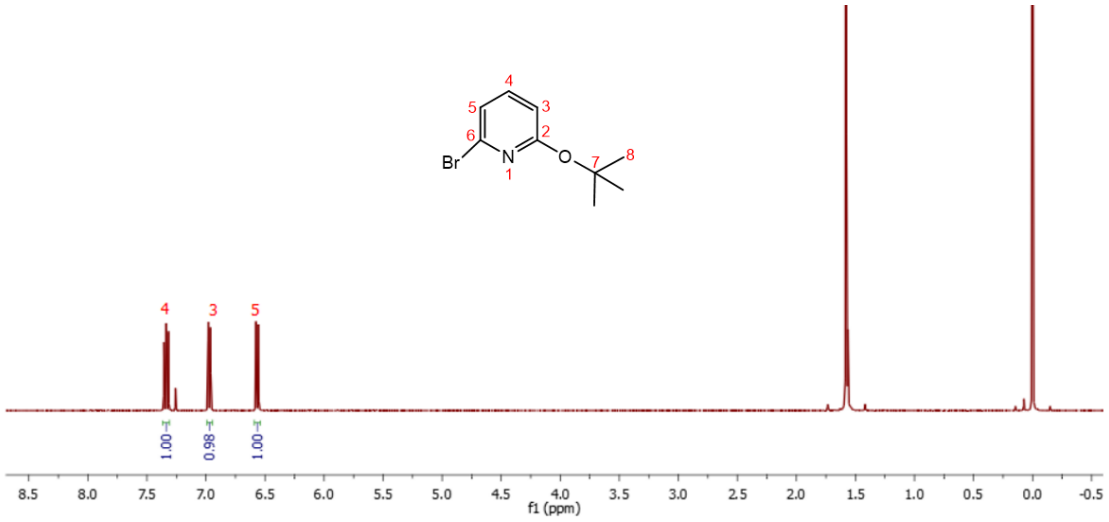

Figure S1 ^{1}H NMR ($CDCl_3$) spectrum of 2-*t*butyloxy-6-bromopyridine.

Potassium-*t*butoxide (1.52 g, 13.6 mmol) was dissolved in dry toluene (20 mL) and added to a stirring solution of 2,6-dibromopyridine (3.22 g, 13.6 mmol) in dry toluene (40 mL) in a 100 mL Schlenk flask. The reaction mixture was left stirring overnight at 80ºC under nitrogen atmosphere, and then allowed to cool to room temperature. The mixture was filtered through a wet pad of celite and the solvent in the filtrate was removed under reduced pressure to reveal a white semi-solid crude product. This was then purified by column chromatography, eluting the product using hexane (100%) as the eluting solvent. Removal of the solvent under reduced pressure and drying *in vacuo* yielded a clear oil product. Yield: (1.64 g, 53%). ^{1}H NMR ($CDCl_3$, δ): 7.34 (dd, ^{3}J = 8.4 Hz, ^{3}J = 7.6 Hz, 1H, H_4), 6.97 (dd, ^{3}J = 7.6 Hz, ^{4}J = 0.8 Hz, 1H, H_5), 6.56 (dd, ^{3}J = 8.4 Hz, ^{3}J = 0.8 Hz, 1H, H_3), 1.58 (s, 1H, H_8). ^{13}C{^{1}H} NMR ($CDCl_3$, δ): 163.0 (s, C_6), 140.0 (s, C_4), 137.6 (s, C_2), 119.5 (s, C_3), 111.4 (s, C_5), 80.87 (s, C_7), 28.40 (s, C_8). FT-IR (ν_{max}/cm^{-1}): 1586.9 (C=N).

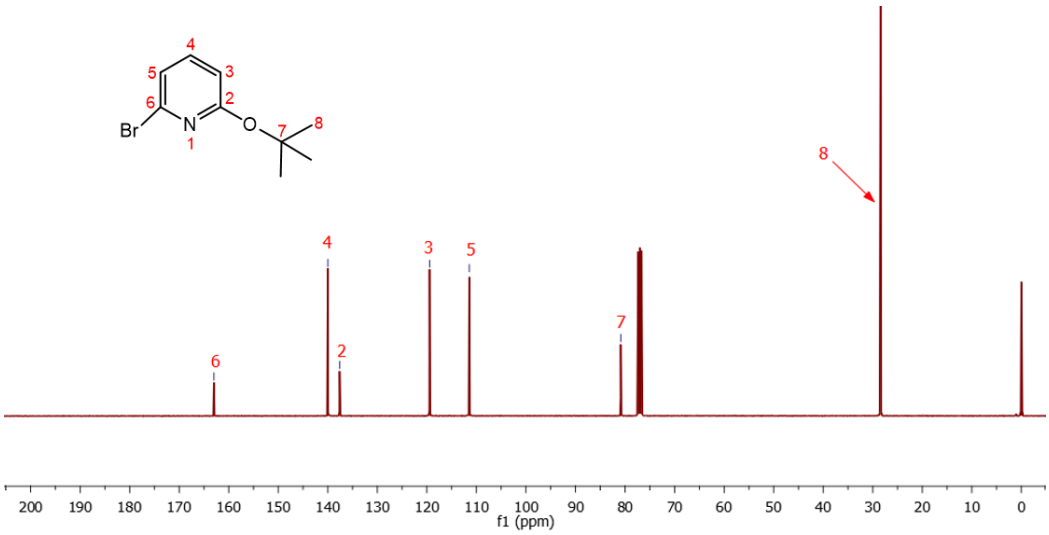

Figure S2 $^{13}C\{^{1}H\}$ NMR ($CDCl_3$) spectrum of 2-*t*butyloxy-6-bromopyridine.

3. Synthesis and Characterisation of 2-*t*butyloxy-6-dicyclohexylphosphinyl-pyridine

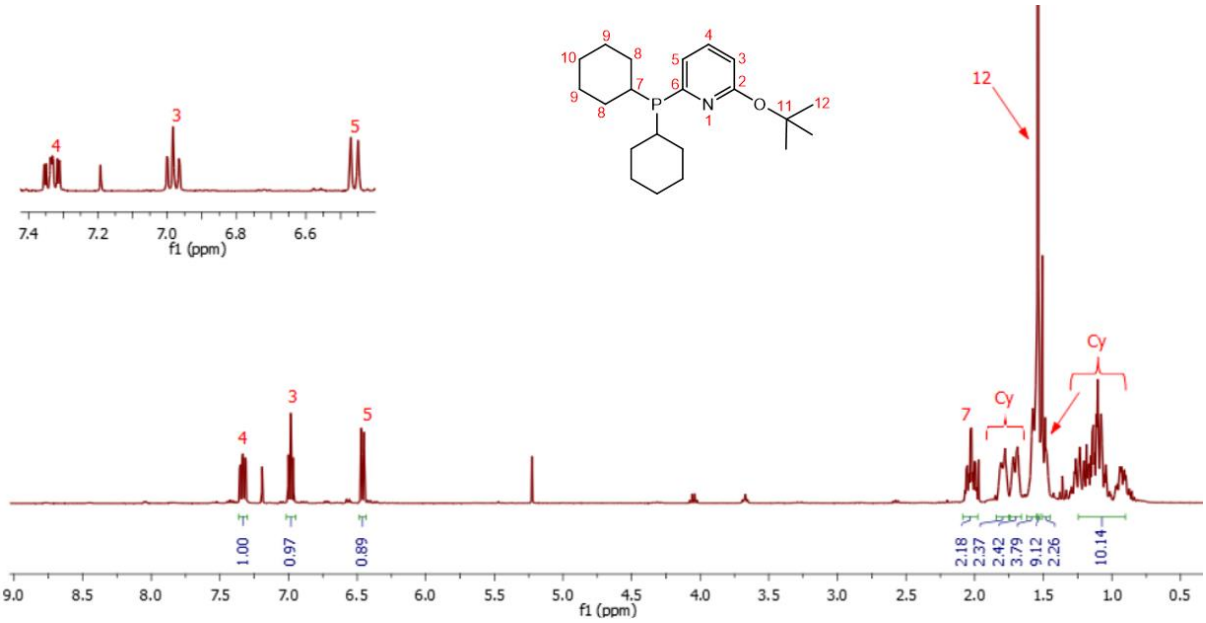

Figure S3 ^{1}H NMR ($CDCl_3$) spectrum of 2-*t*butyloxy-6-dicyclohexylphosphinylpyridine.

2-*t*Butyloxy-6-bromopyridine (1.04 g, 4.52 mmol) was dissolved in dry THF (30 mL) in a 100 mL Schlenk flask, and the solution was cooled to -78°C. To this solution was added n-Butyllithium (1.52 M in hexane, 3.27 mL, 4.97 mmol) dropwise (over 30 min) and the reaction was allowed to continue stirring for 3 hours at -78°C. Chlorodicyclohexylphosphine (1.16 g, 4.97 mmol) was dissolved in dry THF (30 mL) and then cannulated to the stirring solution. The reaction was left stirring to room temperature overnight under nitrogen, after which distilled water (15 mL) was added, and the organic solvent was removed under reduced pressure. An extraction was carried out with ethyl acetate and the organic layer was washed with distilled water,

brine and then filtered over magnesium sulfate. The filtrate was further purified by column chromatography (100% DCM), eluting the product as a clear oil which was collected and dried *in vacuo*. Yield: (1.14 g, 72%). ^{1}H NMR ($CDCl_3$, δ): 7.33 (ddd, ^{3}J = 8.3 Hz, ^{3}J = 7.1 Hz, $^{4}J_{HP}$ = 2.3 Hz, 1H, H_4), 6.98 (td, ^{3}J = 7.0 Hz, ^{4}J = 0.8 Hz, 1H, H_3), 6.46 (ddd, ^{3}J = 8.3 Hz, $^{3}J_{HP}$ = 8.2 Hz, ^{4}J = 1.2 Hz, 1H, H_5), 2.09–1.98 (m, 2H, H_7), 1.84–1.75 (m, 2H, H_{Cy}), 1.75–1.66 (m, 2H, H_{Cy}), 1.62–1.55 (m, 4H, H_{Cy}), 1.54 (s, 9H, H_{12}), 1.51–1.45 (m, 2H, H_{Cy}), 1.24–0.90 (m, 10H, H_{Cy}). ^{13}C{^{1}H} NMR ($CDCl_3$, δ): 163.4 (d, $^{3}J_{PC}$ = 3.6 Hz, C_2), 137.1 (d, $^{1}J_{PC}$ = 23 Hz, C_6), 125.2 (d, $^{3}J_{PC}$ = 4.2 Hz, C_4), 112.8 (d, $^{2}J_{PC}$ = 10 Hz, C_5), 79.18 (s, C_3), 32.77 (br s, Cy), 29.85 (d, J_{PC} = 13.7 Hz, Cy), 29.35 (br s, Cy), 29.73 (s, C_{12}), 28.58 (s, C_{11}), 27.25 (d, J_{PC} = 11.9 Hz, Cy), 26.97 (d, J_{PC} = 8.2 Hz, Cy), 26.41 (br s, Cy). ^{31}P{^{1}H} NMR ($CDCl_3$, δ): 8.39 (s). FT-IR (ν_{max}/cm^{-1}): 1563.7 (C=N). Elemental Anal. Calcd. For: $C_{21}H_{34}NOP$, (%) C: 72.59, H: 9.86, N: 4.03, Found (%) C: 72.68, H: 9.63, N: 3.78. ESI-MS (positive ion-mode), (*m/z*) = 348.25 [M + H]$^{+}$ (calcd. 348.25).

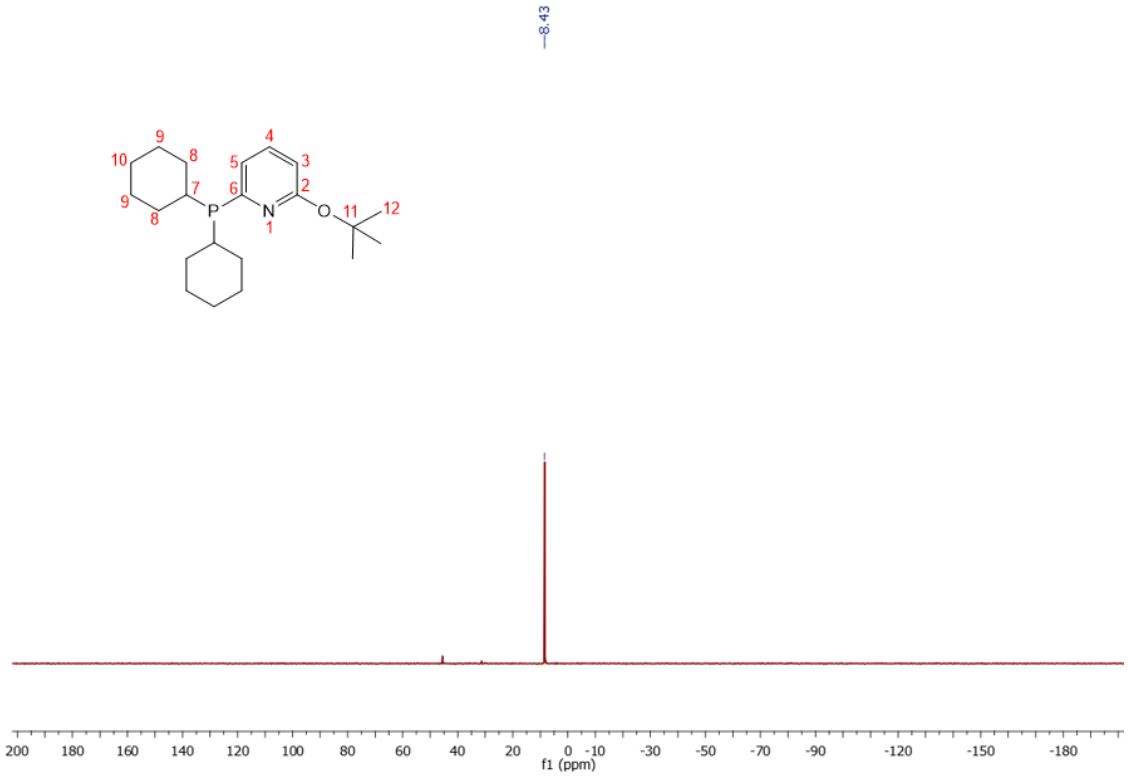

Figure S4 ^{31}P{^{1}H} NMR ($CDCl_3$) spectrum of 2-*t*butyloxy-6-dicyclohexylphosphinylpyridine.

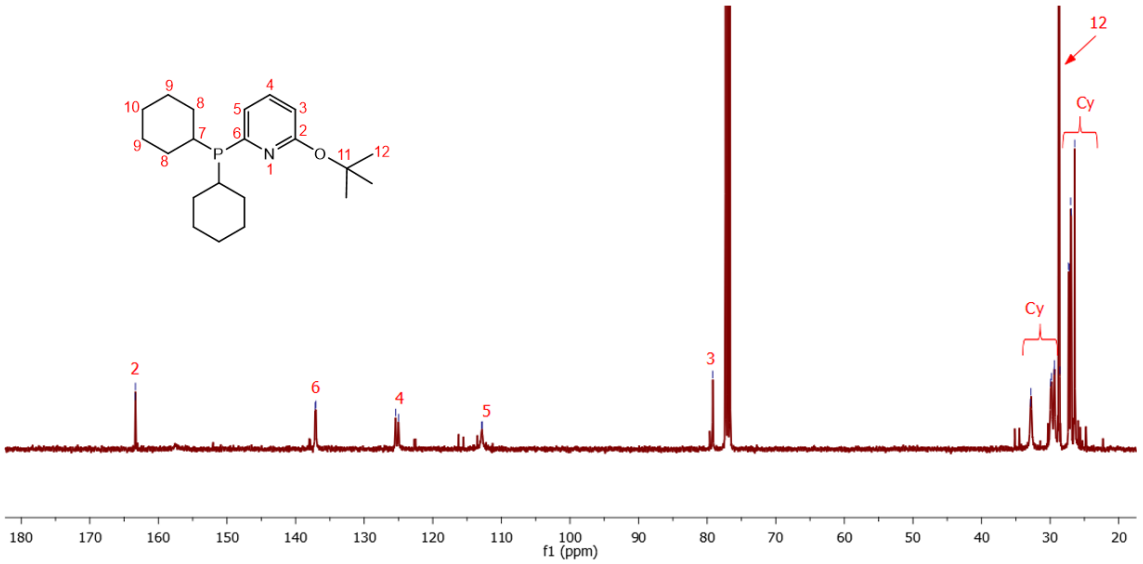

Figure S5 $^{13}C\{^{1}H\}$ NMR ($CDCl_3$) spectrum of 2-*t*butyloxy-6-dicyclohexylphosphinylpyridine.

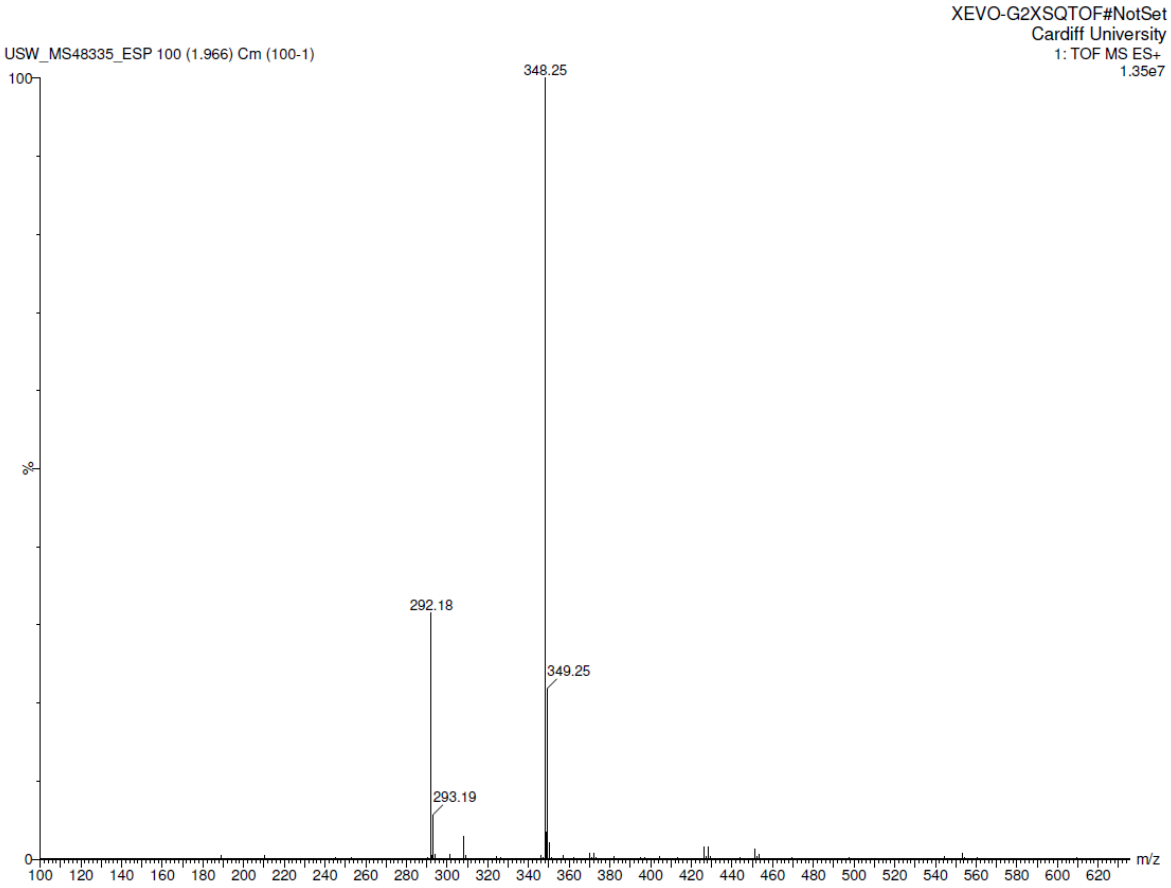

Figure S6 ESI-MS fragmentation pattern of 2-*t*butyloxy-6-dicyclohexylphosphinylpyridine.

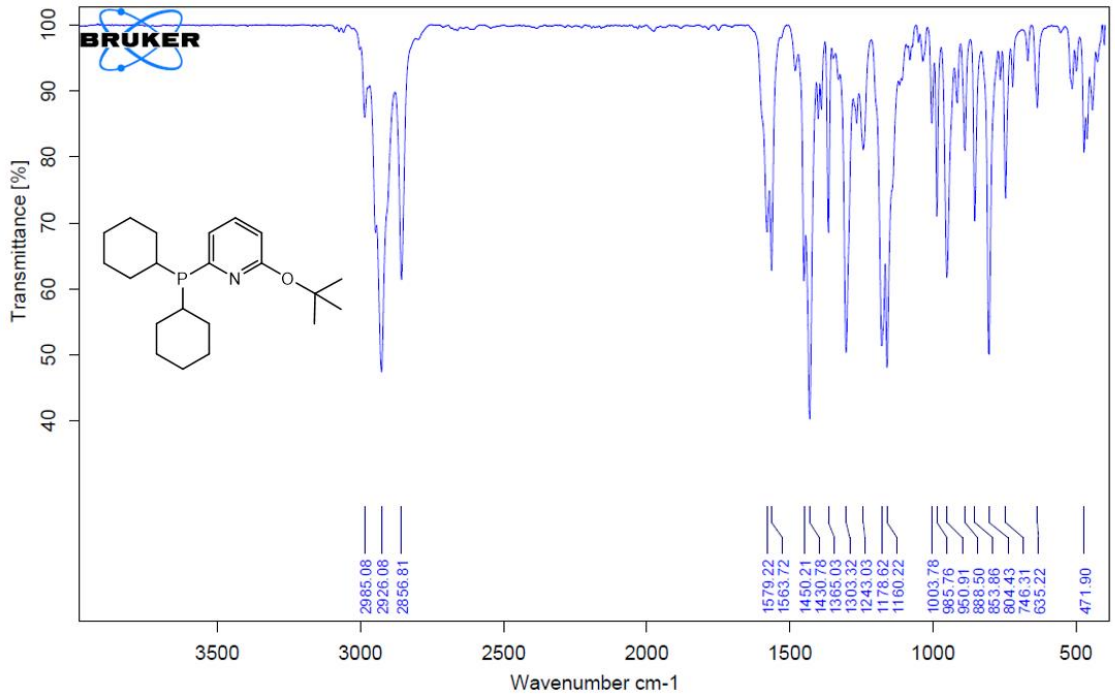

Figure S7 FT-IR spectrum of 2-^{t}butyloxy-6-dicyclohexylphosphinylpyridine.

4. Synthesis and Characterisation of 6-dicyclohexylphosphino-2-pyridone (6-D^{Cy}PPon)

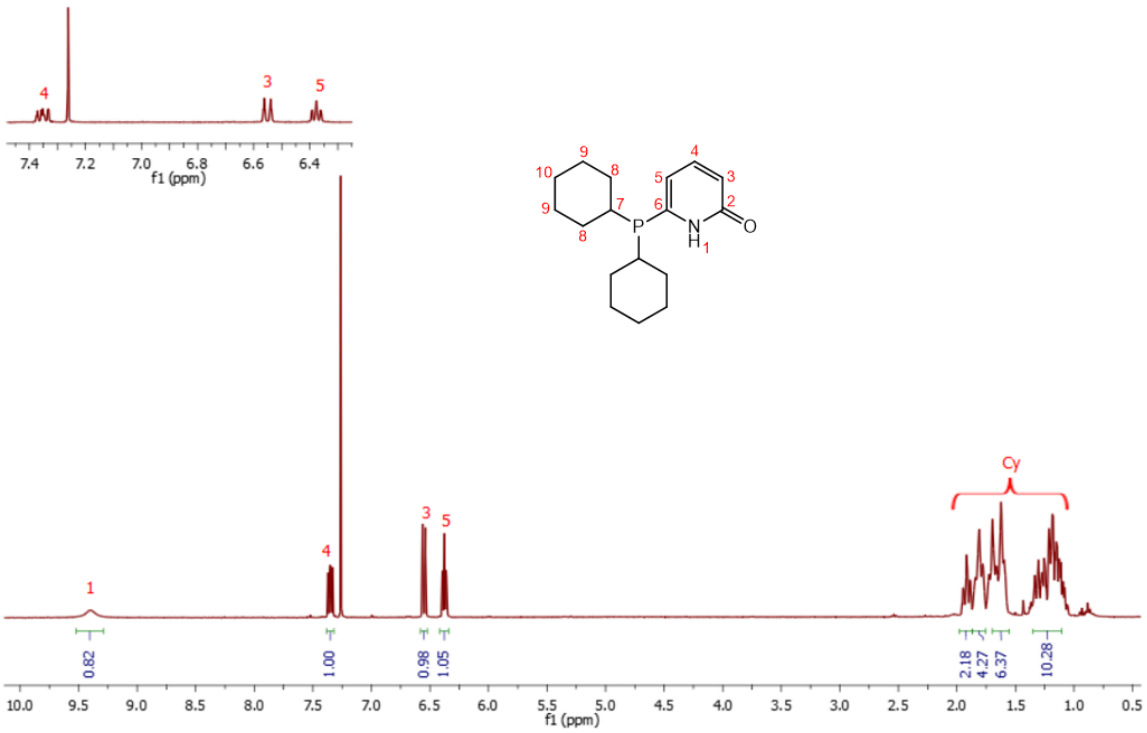

Figure S8 ^{1}H NMR ($CDCl_3$) spectrum of 6-dicyclohexylphosphino-2-pyridone (**6-D^{Cy}PPon**).

Formic acid (15 mL, concentrated) was added dropwise to a 100 mL Schlenk flask containing 2-*t*butyloxy-6-dicyclohexylphosphinylpyridine (1.38 g, 3.97 mmol) kept under nitrogen atmosphere. The reaction was left stirring at room temperature for 4 h, after which distilled water (25 mL) was added, revealing a milky-white solution. The solution was transferred to a separating funnel for extraction using DCM. The organic extracts were combined and washed with brine, then dried over $MgSO_4$ and filtered by gravity. The solvent in the filtrate was removed under reduced pressure, and residual formic acid was removed *via* azeotropic distillation with ethanol, revealing a white solid product which was collected and dried *in vacuo*. Yield: (1.02 g, 88%). ^{1}H NMR ($CDCl_3$, *δ*): 9.40 (br s, 1H, H_1), 7.35 (ddd, ^{3}J = 9.2 Hz, ^{3}J = 6.6 Hz, $^{4}J_{HP}$ = 1.1 Hz, 1H, H_4), 6.55 (dt, ^{3}J = 9.2 Hz, ^{4}J = 1.1 Hz, 1H, H_3), 6.38 (ddd, ^{3}J = 6.8 Hz, $^{3}J_{HP}$ = 6.0 Hz, ^{4}J = 1.2 Hz, 1H, H_5), 1.98–1.87 (m, 2H, H_{Cy}), 1.87–1.75 (m, 4H, H_{Cy}), 1.70–1.56 (m, 6H, H_{Cy}), 1.35–1.10 (m, 10H, H_{Cy}). ^{13}C{^{1}H} NMR ($CDCl_3$, *δ*): 163.4 (s, C_2), 144.7 (d, $^{1}J_{PC}$ = 35.3 Hz, C_6), 139.2 (d, $^{3}J_{PC}$ = 8.6 Hz, C_4), 120.0 (s, C_3), 114.4 (d, $^{2}J_{PC}$ = 23.1 Hz, C_5), 31.46 (d, J_{PC} = 12.1 Hz, Cy), 29.12 (d, J_{PC} = 17.2 Hz, Cy), 28.26 (d, J_{PC} = 7.1 Hz, Cy), 25.90 (d, J_{PC} = 12.9 Hz, Cy), 25.69 (d, J_{PC} = 7.7 Hz, Cy), 25.14 (d, J_{PC} = 1.0 Hz, Cy). ^{31}P{^{1}H} NMR ($CDCl_3$, *δ*): 2.99 (s). FT-IR (ν_{max}/cm^{-1}): 2855.8 (N–H), 1648.8 (C=O). Elemental Anal. Calcd. For: $C_{17}H_{26}NOP$, (%) C: 70.08, H: 8.99, N: 4.81, Found (%) C: 69.65, H: 8.96, N: 4.49. ESI-MS (positive ion-mode), (*m/z*) = 292.18 $[M + H]^+$ (calcd. 292.18).

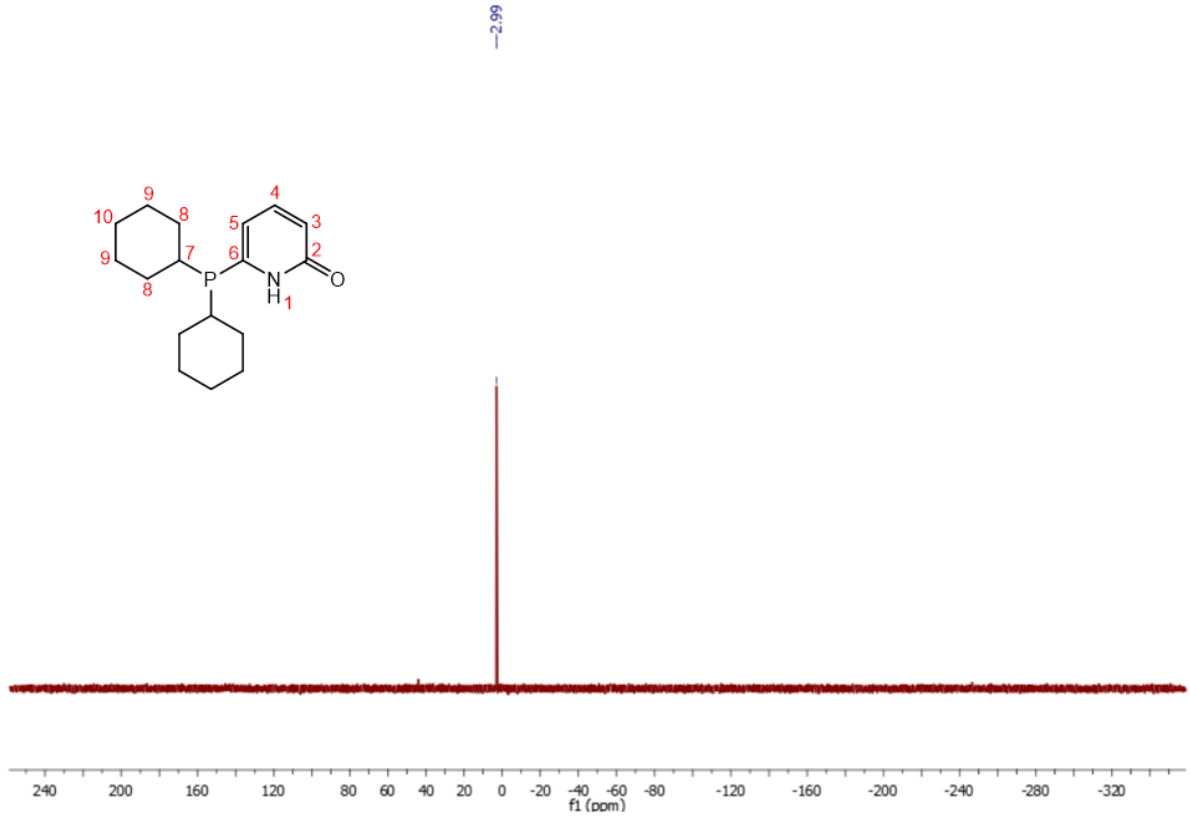

Figure S9 ^{31}P{^{1}H} NMR ($CDCl_3$) spectrum of 6-dicyclohexylphosphino-2-pyridone (**6-D^{Cy}PPon**).

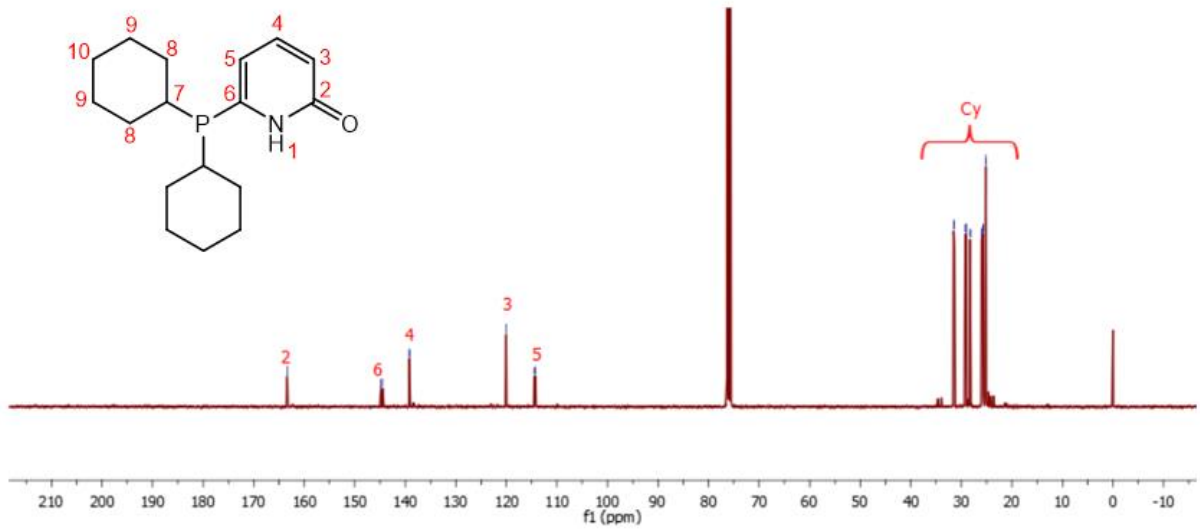

Figure S10 $^{13}C\{^{1}H\}$ NMR ($CDCl_3$) spectrum of 6-dicyclohexylphosphino-2-pyridone (**6-D^{Cy}PPon**).

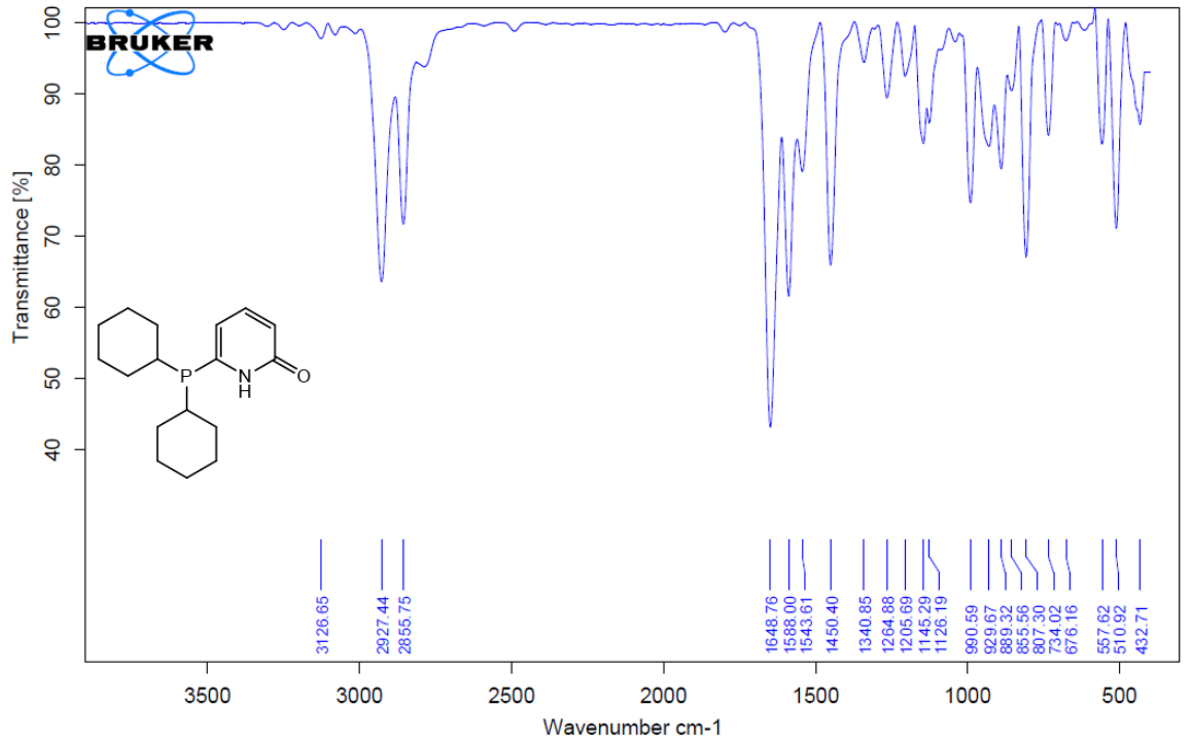

Figure S11 FT-IR spectrum of 6-dicyclohexylphosphino-2-pyridone (**6-D^{Cy}PPon**).

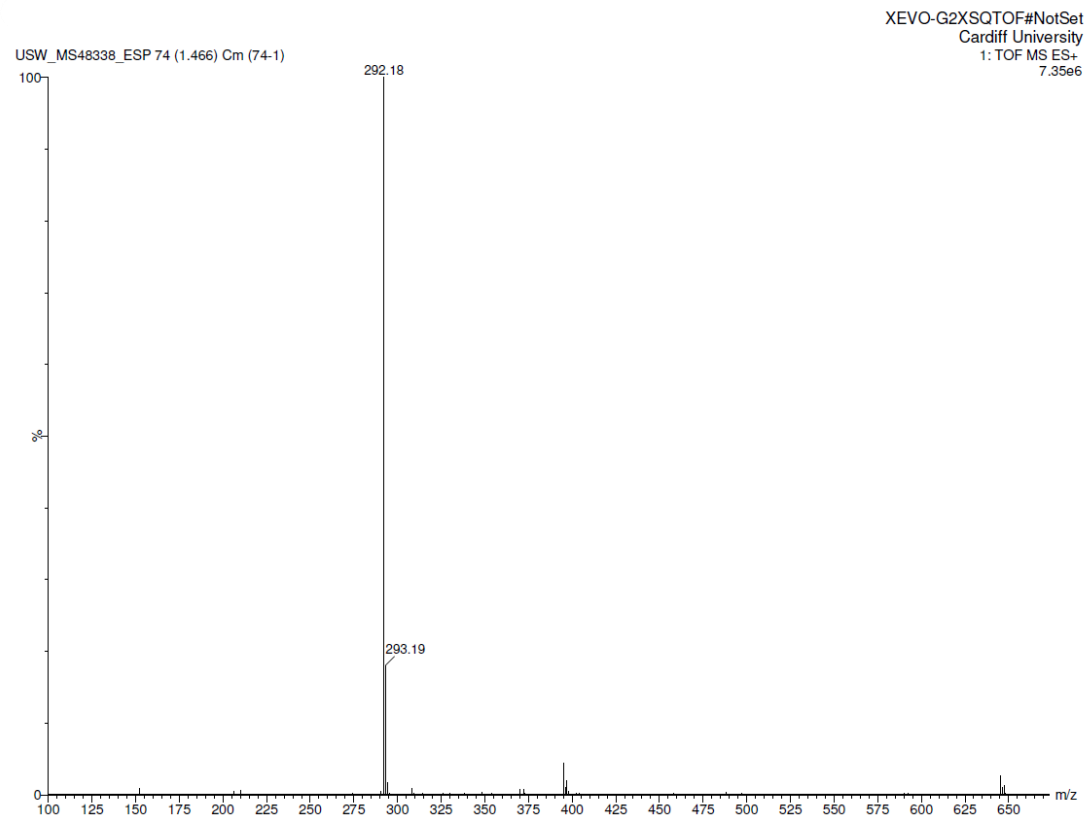

Figure S12 ESI-MS fragmentation pattern of 6-dicyclohexylphosphino-2-pyridone (**6-D^{Cy}PPon**).

5. Synthesis and Characterisation of [Ir(κ^2-*P,N*-6-D^{Cy}Pon*)(COD)] (1)

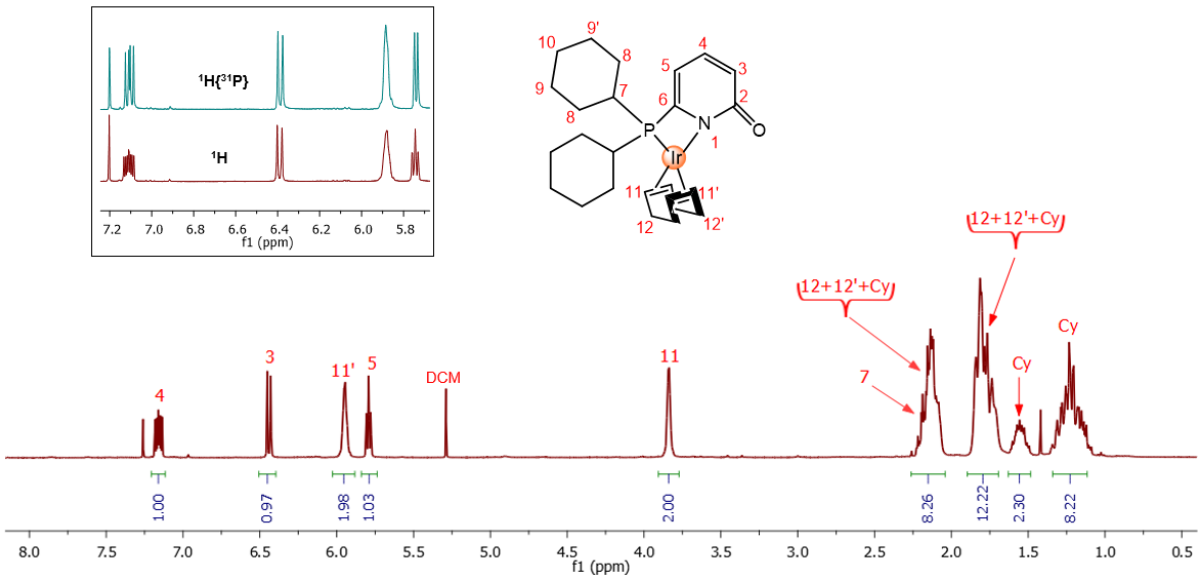

Figure S13 ^{1}H NMR ($CDCl_3$) spectrum of [Ir(κ^2-*P,N*-**6-D^{Cy}Pon***)(COD)] (**1**).

6-Dicyclohexylphosphinylpyridone (0.250 g, 0.859 mmol) was dissolved in dry DCM (10 mL) under nitrogen atmosphere, and added dropwise to a stirring solution of

iridium dimer $[Ir(COD)OMe]_2$ (0.285 g, 0.429 mmol) in DCM (10 mL). The solution was left stirring overnight at room temperature under nitrogen atmosphere. The solvent of the reaction was then removed *in vacuo* to reveal a reddish-orange solid product which was collected and dried *in vacuo*. Yield: (0.458 g, 90%). ^{1}H NMR ($CDCl_3$, δ): 7.10 (ddd, $^{3}J_{HH}$ = 9.1 Hz, $^{3}J_{HH}$ = 6.5 Hz, $^{4}J_{HP}$ = 3.6 Hz, 1H, H_4), 6.38 (dd, $^{3}J_{HH}$ = 9.2 Hz, $^{4}J_{HH}$ = 0.8 Hz, 1H, H_3), 5.89 (br s, 1H, $H_{11',trans\text{-}P}$), 5.73 (ddd, $^{3}J_{HH}$ = 6.4 Hz, $^{3}J_{HP}$ = 5.2 Hz, $^{4}J_{HH}$ = 1.0 Hz, 1H, H_5), 3.78 (br s, 2H, $H_{11,trans\text{-}N}$), 2.17–1.99 (m, 8H, $H_{7+12+12'+Cy}$), 1.82–1.63 (m, 12H, $H_{12+12'+Cy}$), 1.57–1.44 (m, 2H, H_{Cy}), 1.30–1.03 (m, 8H, H_{Cy}). ^{13}C{^{1}H} NMR ($CDCl_3$, δ): 169.2 (d, $^{3}J_{PC}$ = 14 Hz, C_2), 162.6 (d, $^{1}J_{PC}$ = 53.5 Hz, C_6), 135.6 (d, $^{3}J_{PC}$ = 7.9 Hz, C_4), 120.6 (d, $^{4}J_{PC}$ = 2.5 Hz, C_3), 109.8 (d, $^{2}J_{PC}$ = 3.1 Hz, C_5), 88.01 (d, $^{2}J_{PC}$ = 10.6 Hz, $C_{cod\text{-}11',trans\text{-}P}$), 55.24 (s, $C_{cod\text{-}11,trans\text{-}N}$), 31.83 (d, J_{PC} = 3.0 Hz, $C_{cod\text{-}12,trans\text{-}N}$), 30.27 (d, $^{2}J_{PC}$ = 23.3 Hz, C_7), 29.77 (d, J_{PC} = 1.4 Hz, Cy), 28.16 (d, $^{1}J_{PC}$ = 3.4 Hz, Cy), 27.94 (s, $C_{cod\text{-}12',trans\text{-}P}$), 25.65 (dd, J_{PC} = 16.56 Hz, J_{PC} = 13.94 Hz, Cy), 24.94 (s, Cy). ^{31}P{^{1}H} NMR ($CDCl_3$, δ): –31.53 (s). FT-IR (ν_{max}/cm^{-1}): 1622.3 (C=O). Elemental Anal. Calcd. For: $C_{25}H_{37}NOPIr$, (%) C: 50.83, H: 6.31, N: 2.31, Found (%) C: 50.17, H: 6.04, N: 2.90. ESI-MS (positive ion-mode), (*m/z*) = 592.23 $[M + H]^+$ (calcd. 592.22).

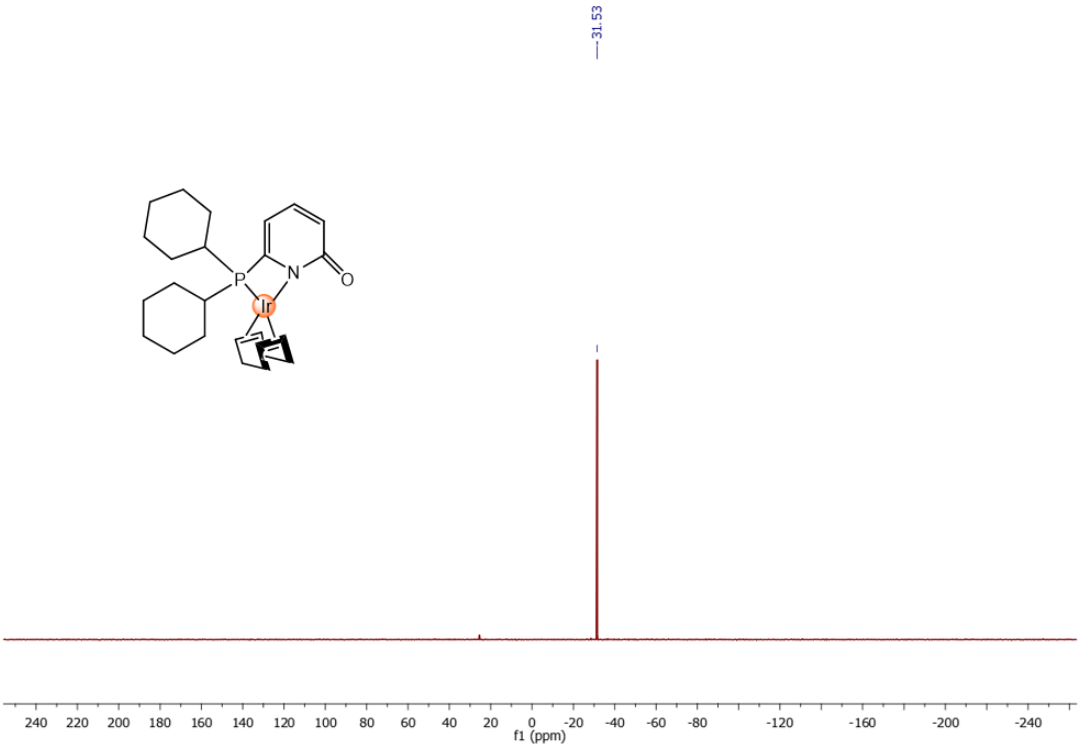

Figure S14 ^{31}P{^{1}H} NMR ($CDCl_3$) spectrum of [Ir(κ^2-*P,N*-**6-D^{Cy}Pon*)**(COD)] (**1**).

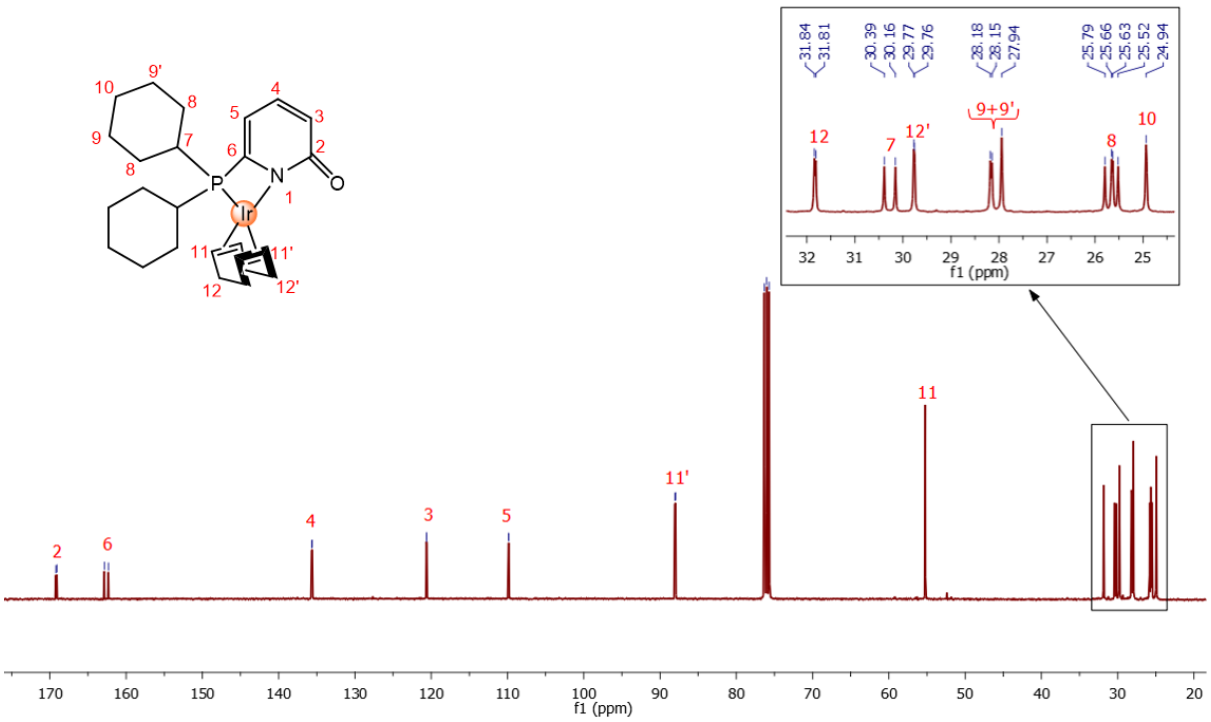

Figure S15 $^{13}C\{^{1}H\}$ NMR ($CDCl_3$) spectrum of [Ir(κ²-*P,N*-**6-D^{Cy}Pon*)**(COD)] (**1**).

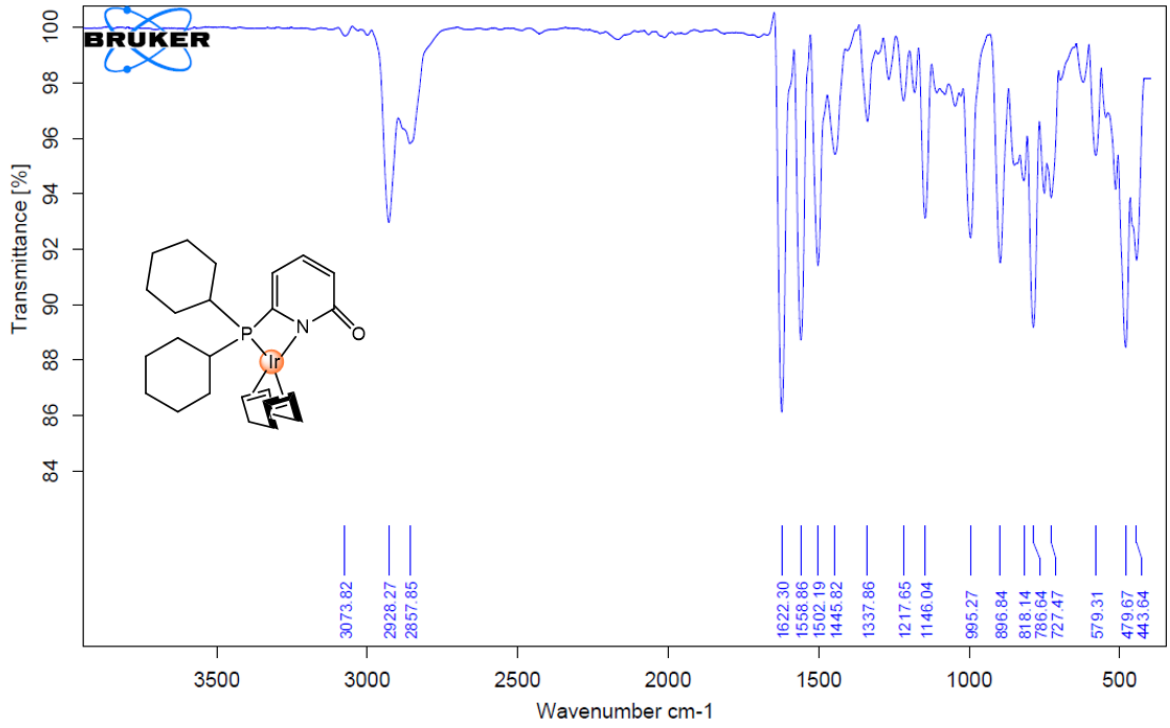

Figure S16 FT-IR spectrum of [Ir(κ²-*P,N*-**6-D^{Cy}Pon*)**(COD)] (**1**).

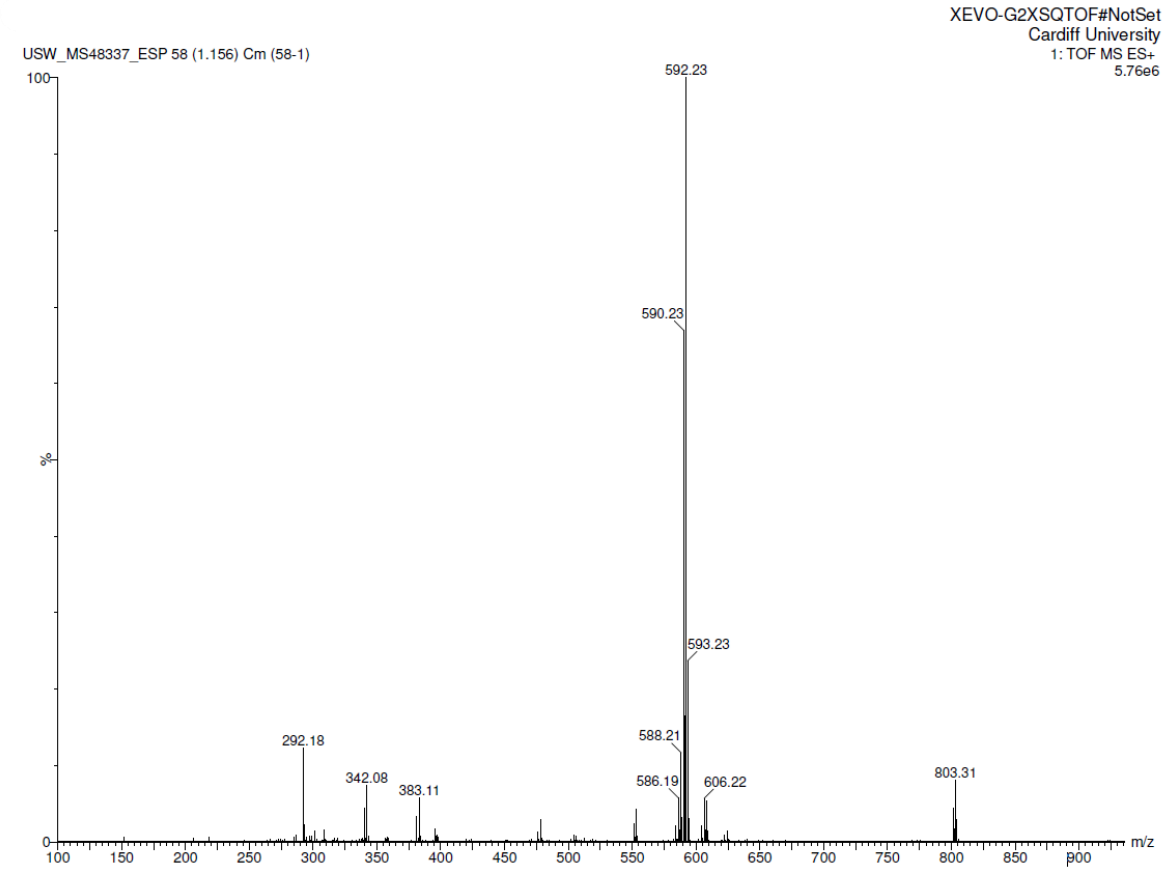

Figure S17 ESI-MS fragmentation pattern of [Ir(κ^2-*P,N*-**6-D^{Cy}Pon*)**(COD)] (**1**).

6. Catalytic hydrogenation of CO_2 to formate salt using complex 1

In a nitrogen filled glovebox, complex **1** (5.90 x 10^{-3} g, 0.010 mmol or 9.8 x 10^{-4} g, 1.66 x 10^{-3} mmol), DBU (between 0 – 10,000 equivalents) [see Table S1 below for details on each run], and THF (5 mL) were added to a 50 mL high-pressure autoclave reactor equipped with a magnetic stirrer bar. The charged reactor was then placed in the fume hood and pressurised with CO_2 gas while stirring to reach the equilibration pressure. This is to allow the DBU within the mixture to react to form the DBU•CO_2 adduct.[17] This was followed by H_2 gas and stirred at the room temperature of the laboratory (20 °C ± 2 °C). After stirring for the desired time, the pressure in the reactor was carefully released. DMF (equimolar to DBU) was then added as an internal standard into the reaction mixture. The reaction mixture was then analysed by ^{1}H NMR with a few drops of D_2O to lock the signals.

Table S1 Showing quantities of catalyst and base used for the experiments.

Entry[a]	Catalyst		DBU		
	mmol	mass	equiv.	mmol	Mass
1 – 3	0.01 mmol	5.9 x 10^{-3} g	500	5.00 mmol	0.7612 g
4	0.01 mmol	5.9 x 10^{-3} g	0	0	0
5	0.01 mmol	5.9 x 10^{-3} g	5000	50.00 mmol	7.612 g
6[b] & 7[b]	1.66 x 10^{-3} mmol	9.8 x 10^{-4} g	10000	16.66 mmol	2.5373 g

[a] All entries correlate with Table 1 in main article. [b] The reactions involving 10000 equiv., were carried out on a six-fold lower scale (quantities divided by 6), with the exception of THF, to circumvent requirement for large quantities of DBU base.

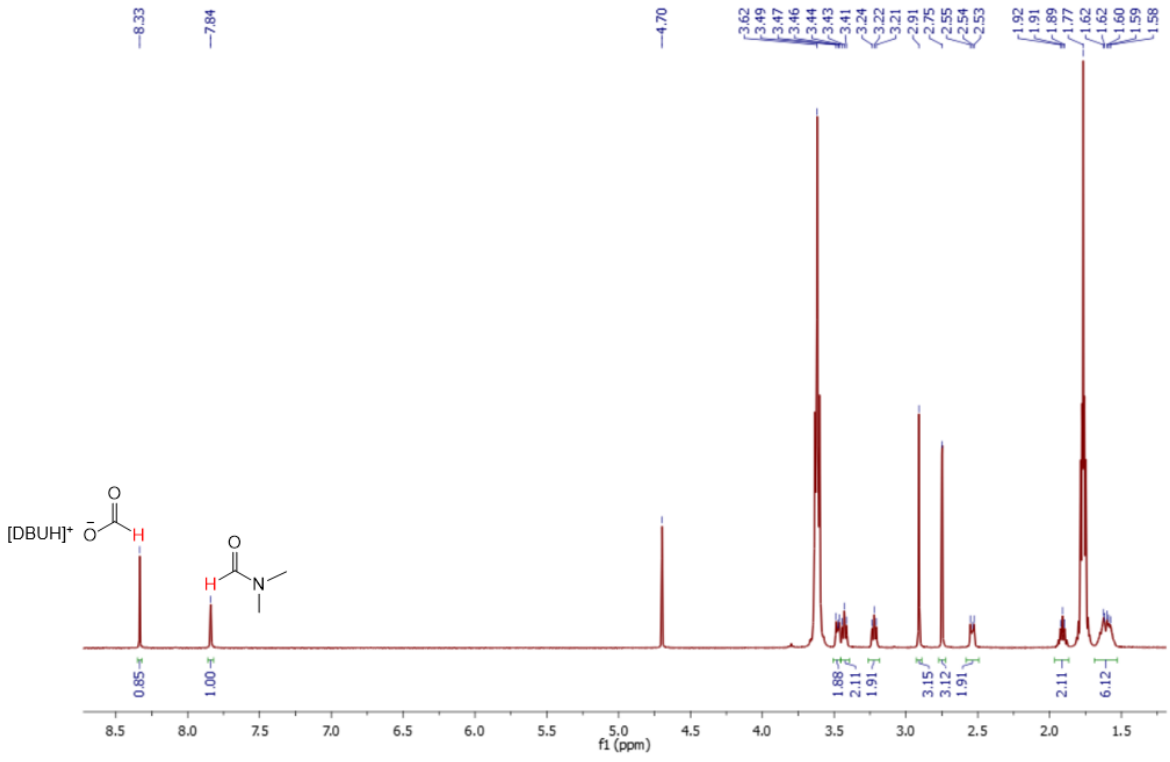

Figure S18 A representative ^{1}H NMR (D_2O) spectrum of a crude catalytic reaction mixture used for computing the TON (table 1, entry 2 in main article).

7. High pressure NMR spectroscopy studies: reactivity of complex 1 with H_2

Complex **1** (5.9 x 10^{-3} g, 0.01 mmol) was dissolved in benzene-d_6 (0.3 mL) in a high-pressure NMR tube, which was then pressurised with 1 bar H_2 and spectra were recorded for ^{1}H and $^{31}P\{^{1}H\}$ NMR within 10 minutes. The NMR tube was then placed under vacuum to remove the H_2 in the headspace, and filled with nitrogen atmosphere and then spectra were recorded over time.

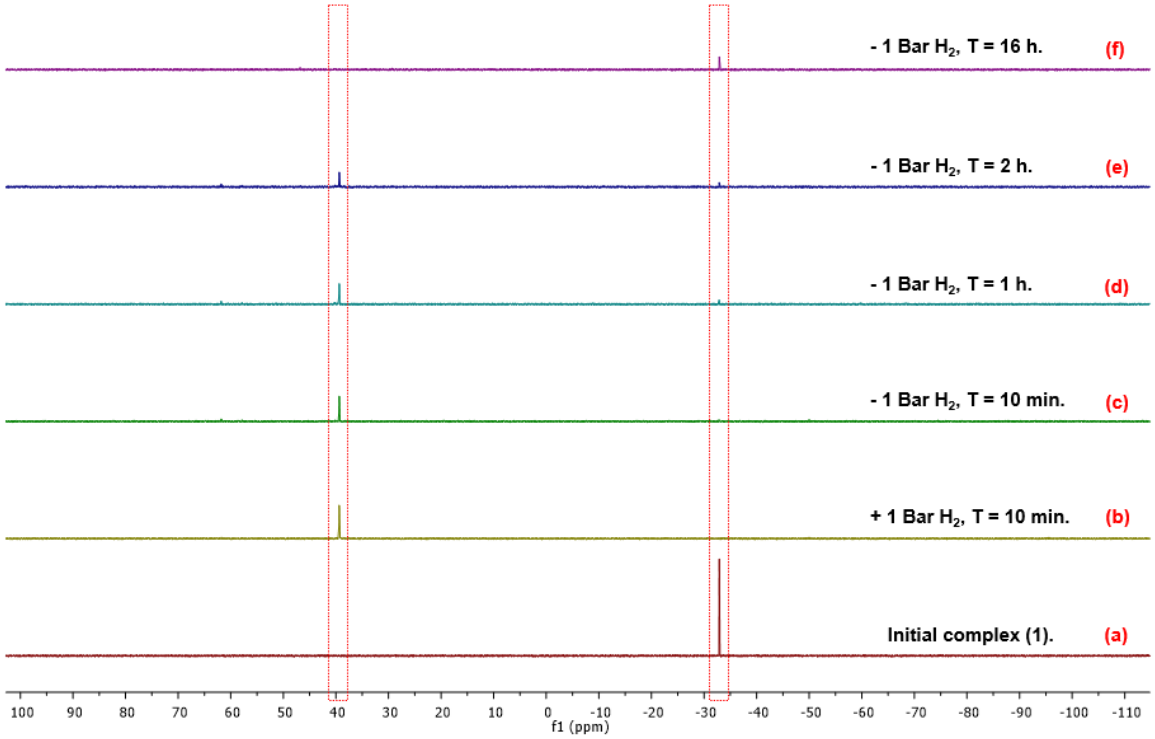

Figure S19 Stacked $^{31}P\{^{1}H\}$ NMR (C_6D_6) spectra of **1** illustrating room temperature reversible reactivity with H_2.

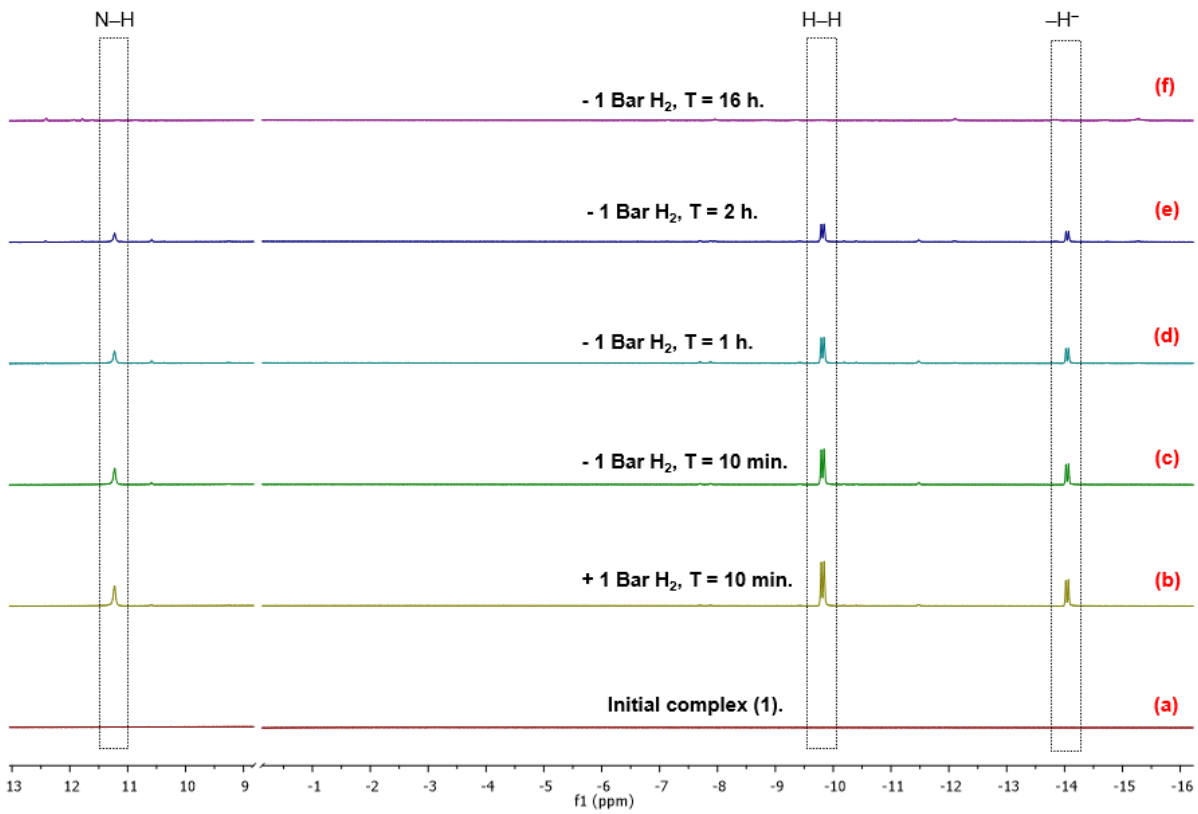

Figure S20 Stacked selected regions of ^{1}H NMR (C_6D_6) spectra of **1** illustrating room temperature reversible reactivity with H_2.

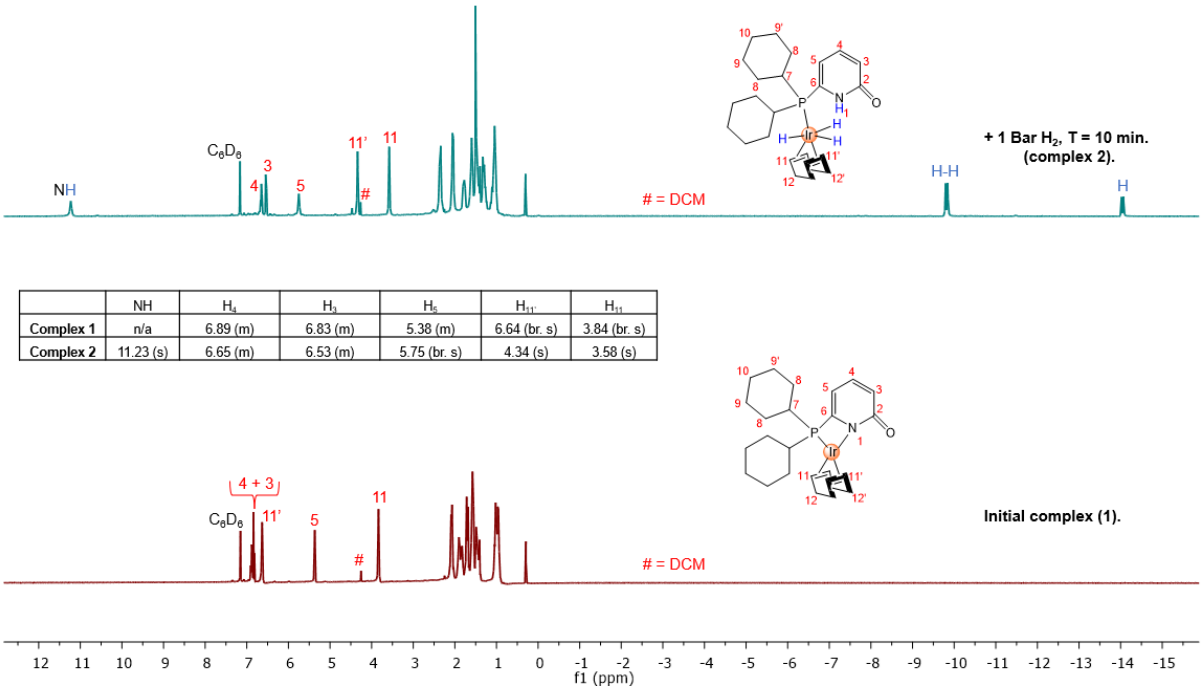

	NH	H_4	H_3	H_5	$H_{11'}$	H_{11}
Complex 1	n/a	6.89 (m)	6.83 (m)	5.38 (m)	6.64 (br. s)	3.84 (br. s)
Complex 2	11.23 (s)	6.65 (m)	6.53 (m)	5.75 (br. s)	4.34 (s)	3.58 (s)

Figure S21 Full range stacked ^{1}H NMR (C_6D_6) spectra illustrating room temperature reactivity of complex **1** with H_2 to form complex **2**. Inset table: showing differences in chemical shifts of complexes **1** and **2**.

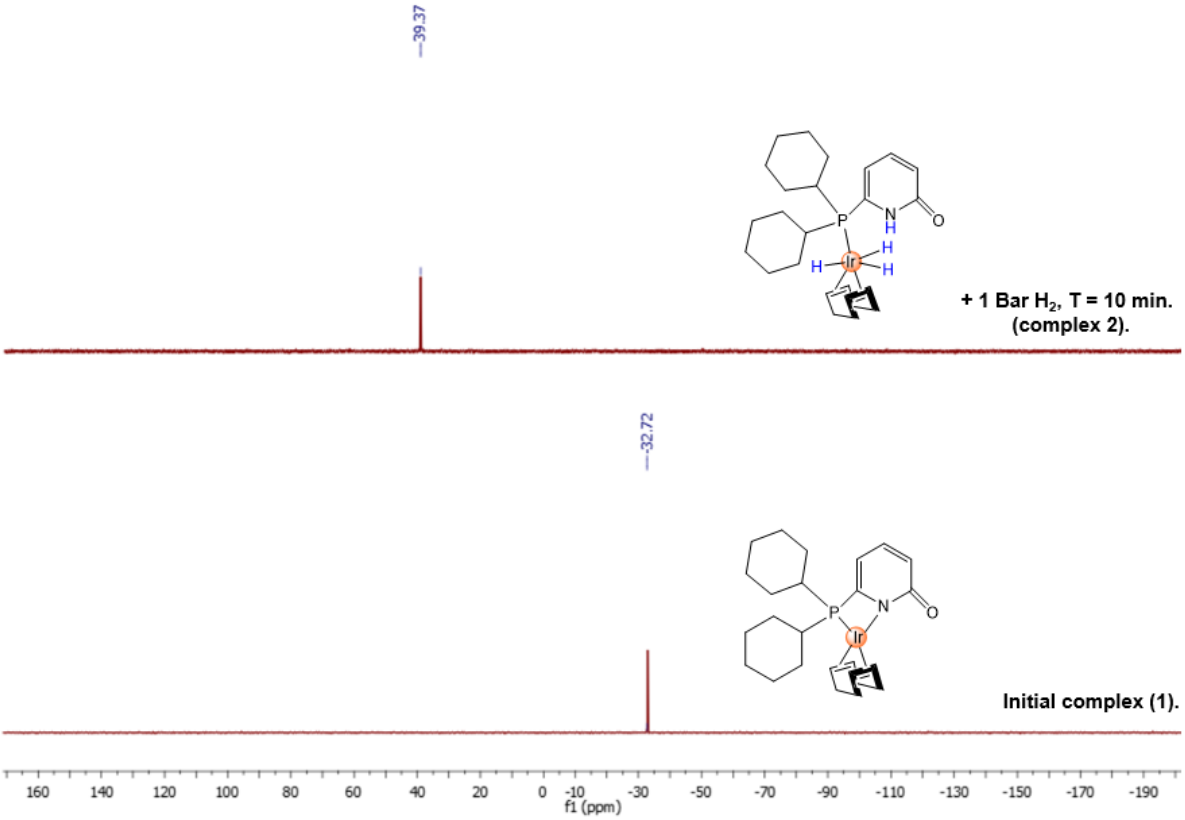

Figure S22 Stacked $^{31}P\{^{1}H\}$ NMR (C_6D_6) spectra illustrating room temperature reactivity of complex **1** with H_2 to form complex **2**.

8. Crystallographic data collection, reduction, and structure solution refinement

CCDC number 2309375, (NCS **2023ncs0208r1**), contain supplementary crystallographic data for complex **1**. This data can be obtained free of charge from the Cambridge Crystallographic Data Centre via www.ccdc.cam.ac.uk/data_request/cif.

Details for complex 1

Single orange block-shaped crystals of **1** were obtained by recrystallisation from a concentrated THF solution. A suitable crystal 0.15×0.10×0.09 mm^3 was selected and mounted on a MITIGEN holder in oil on a Rigaku FRE+ diffractometer with Arc) Sec VHF Varimax confocal mirrors, a UG2 goniometer and HyPix 6000HE detector. The crystal was kept at a steady T = 100(2) K during data collection. The data was processed using the CrysAlisPro 1.171.42.94a program.[18] The structure was solved with the ShelXT 2018/2[19] structure solution program using the using dual methods solution method and by using Olex2 1.5-alpha[20] as the graphical interface. The model was refined with olex2.refine 1.5-alpha[21] using full matrix least squares minimisation on F^2 minimisation. All non-hydrogen atoms were refined anisotropically. Hydrogen atom positions were calculated geometrically and refined using the riding model.
Additional refinement details: The COD ligand has been modelled as partially disordered (56:44). 1,2 and 1,3 equal distance geometrical restraints have been applied to all equivalent atom pairs of the disorder components.
Experimental absorption process details: CrysAlisPro 1.171.42.94a (Rigaku OD, 2023) using spherical harmonics, implemented in SCALE3 ABSPACK scaling algorithm.

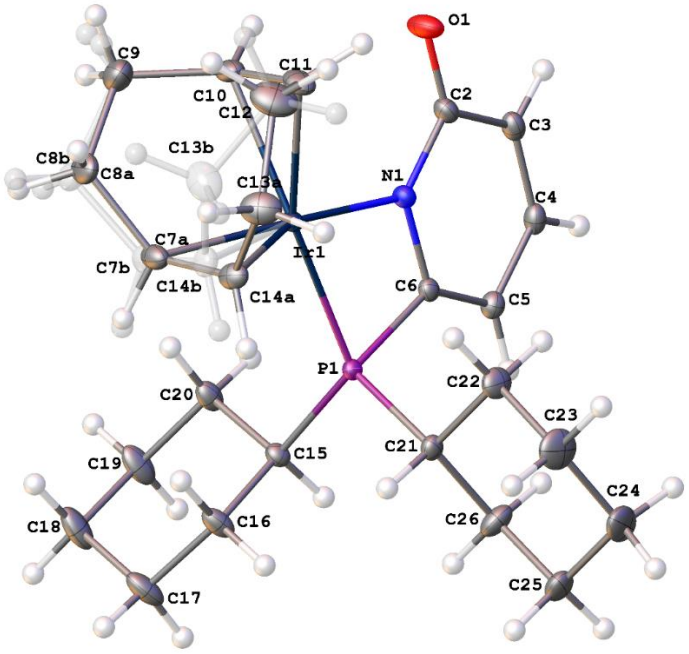

Figure S23 Crystal structure of [Ir(κ²-*P,N*-**6-D^{Cy}Pon*)**(COD)] (**1**), highlighting disorder in the COD unit. The minor component is in grey.

Table S1 X-ray data collection parameters for complex **1**.

Compound	**1**
CCDC No:	2309375
Formula	$C_{25}H_{37}IrNOP$
Dcalc./ g cm^{-3}	1.715
μ/mm^{-1}	5.920
Formula Weight	590.768
Colour	orange
Shape	block-shaped
Size/mm^3	0.15×0.10×0.09
T/K	100(2)
Crystal System	monoclinic
Space Group	$P2_1/n$
a/Å	10.3796(1)
b/Å	16.1116(1)
c/Å	14.0850(1)
α/°	90
β/°	103.693(1)
γ/°	90
V/Å^3	2288.52(3)
Z	4
Z'	1
Wavelength/Å	0.71075
Radiation type	Mo K_α
Q_{min}/°	1.95
Q_{max}/°	36.18
Measured Refl's.	181325
Indep't Refl's	10543
Refl's I≥2 *s* (I)	9721
R_{int}	0.0416
Parameters	299
Restraints	30
Largest Peak	1.5069
Deepest Hole	-1.0295
GooF	1.0456
wR_2 (all data)	0.0406
wR_2	0.0395
R_1 (all data)	0.0236
R_1	0.0194
Flack Parameter	-
Hooft Parameter	-

Table S2 Selected bond distances (Å) for complex **1**.

Atom	Atom	Length/Å
Ir1	P1	2.2975(3)
Ir1	N1	2.0768(12)
Ir1	C7a	2.117(8)
Ir1	C10	2.1864(14)
Ir1	C11	2.1757(15)
Ir1	C14a	2.138(5)
P1	C6	1.8284(14)
P1	C15	1.8340(13)
P1	C21	1.8337(14)
O1	C2	1.2412(18)
N1	C2	1.3946(17)
N1	C6	1.3801(18)
C2	C3	1.452(2)
C3	C4	1.362(2)
C4	C5	1.419(2)
C5	C6	1.3661(19)
C7a	C8a	1.521(8)
C7a	C14a	1.423(8)
C8a	C9	1.528(4)
C9	C10	1.515(2)
C10	C11	1.396(2)
C11	C12	1.510(3)
C12	C13a	1.535(4)
C13a	C14a	1.515(6)

Numbering scheme is used as received from the crystallography data (see Figures 3 and 4 in main article).

Table S3 Selected bond angles (°) for complex **1**.

Atom	Atom	Atom	Angle/°
N1	Ir1	P1	69.13(3)
C7a	Ir1	P1	105.4(2)
C7a	Ir1	N1	163.67(15)
C10	Ir1	P1	161.45(5)
C10	Ir1	N1	99.15(5)
C10	Ir1	C7a	81.8(2)
C11	Ir1	P1	155.52(5)
C11	Ir1	N1	100.26(5)
C11	Ir1	C7a	90.35(19)
C11	Ir1	C10	37.32(6)
C14a	Ir1	P1	98.06(12)
C14a	Ir1	N1	154.32(13)
C14a	Ir1	C7a	39.07(19)
C14a	Ir1	C10	98.05(13)
C14a	Ir1	C11	82.31(14)
C6	P1	Ir1	84.13(4)
C15	P1	Ir1	123.26(5)
C15	P1	C6	110.29(6)
C21	P1	Ir1	119.44(5)
C21	P1	C6	110.06(6)
C21	P1	C15	106.65(6)
C2	N1	Ir1	133.13(10)
C6	N1	Ir1	105.63(8)
C6	N1	C2	120.91(12)
N1	C2	O1	121.44(13)
C3	C2	O1	123.25(13)
C3	C2	N1	115.30(12)
C4	C3	C2	122.40(13)
C5	C4	C3	120.58(13)
C6	C5	C4	116.76(13)
N1	C6	P1	100.77(9)
C5	C6	P1	135.18(11)
C5	C6	N1	124.01(12)
C8a	C7a	Ir1	113.3(4)
C14a	C7a	Ir1	71.3(4)
C14a	C7a	C8a	123.4(5)
C9	C8a	C7a	114.9(4)
C10	C9	C8a	112.39(17)
C10	C9	C8b	116.83(18)
C9	C10	Ir1	110.37(10)
C11	C10	Ir1	70.93(9)
C11	C10	C9	124.66(16)
C10	C11	Ir1	71.76(9)
C12	C11	Ir1	110.89(11)
C12	C11	C10	125.21(16)
C13a	C12	C11	115.99(17)
C14a	C13a	C12	112.7(3)
C7a	C14a	Ir1	69.7(3)
C13a	C14a	Ir1	111.3(3)
C13a	C14a	C7a	124.4(4)

Numbering scheme is used as received from the crystallography data (see Figures 3 and 4 in main article).

9. Computational Details

All DFT calculations undertaken using the ORCA 4.2.1 computational software.[22] Optimisations and analytical frequency calculations were performed at the B97-D3/def2-TZVP level of theory[23-25] with further solvated energy evaluations at the RIJCOSX-wB97M-V/def2-tzvpp level of theory,[26,27] for calculation of the solvation free energy differences. All calculation included the *Resolution of Identity* approximation to reduce computational cost.[28] Solvation correction was implemented with the SMD model derived to represent benzene and THF environments.[29] Numerical precision integration grids were increase beyond the default settings, during optimisations to *Grid4* for the SCF step *Grid5* for the final energy evaluation, and further to *Grid6* for the NMR calculations. NMR predictions were calculated with the TPSSh functional,[30] with the specially derived NMR specific pcS-2 basis set by Jensen.[31] This choice of methodology has been shown to give good predictions at an affordable computational expense.[32] Due to the relativistic nature of iridium the SARC-ZORA-TZVPP basis set was used for the metal centre.[33] Calculations not accounting for relativistic effects did not give reliable predictions.

Graphical visualisation and structural analysis performed from the DFT calculations using Avogadro 1.2.0.[34]

ORCA - xyz coordinates for Complex 2

Ir	-3.01217187798878	-1.85481455874740	-2.07115335151942
P	-0.96320937318143	-2.70493821873981	-2.48602538107660
C	-0.47886311118750	-2.93592268634846	-4.23455966733109
C	-0.62611528815187	-4.35223689959411	-1.75293502742202
H	-1.23353341672822	-3.58314056014649	-4.68833270260594
H	0.50626736117256	-3.40090301761486	-4.33212056183354
H	-0.49144252467817	-1.97486904548892	-4.75345309898109
H	-1.34228498327793	-5.06581710053697	-2.16983020811526
H	-0.78524108810335	-4.29286827798339	-0.67378791175583
H	0.39809171345955	-4.67518060612439	-1.96273258722841
N	0.18824230045862	-1.20139476000055	-0.53692589320014
C	0.41985818802496	-1.70927154846786	-1.77956051178001
C	1.62704861206434	-1.47063795202282	-2.38696703266711
H	1.83980160067984	-1.86296433336540	-3.37243192330654
C	2.59632708282456	-0.69416506968482	-1.69292584486919
H	3.55343074501299	-0.49904190291801	-2.17289919469675
C	2.34871640568102	-0.18881923478766	-0.44712308507060

H	3.07782084321750	0.41420786901533	0.08369417358115
C	1.07885917830653	-0.40534706398590	0.22131519506757
O	0.73650519410837	0.03347670230389	1.31498574891906
C	-4.44154312745919	0.23995812911326	-0.26937746233292
C	-3.47485486414800	1.13692002830482	-1.07012170992171
C	-2.49695567290710	0.36901482474256	-1.95072392282578
C	-2.75269535664488	0.03414529965932	-3.29006596425004
H	-1.45379928605729	0.46444294107985	-1.66741972265111
H	-1.88675879213400	-0.07488259763905	-3.94070665739197
C	-4.78258558348784	-1.06958479749005	-0.95020643577218
C	-4.03858062938738	0.34007252207923	-4.03121402322170
C	-5.15475110552359	-1.20039429085533	-2.29931411615027
H	-4.05933580712780	1.40320816500243	-4.32200933801399
C	-5.31557954022993	-0.01536571472069	-3.24393408415628
H	-4.02781815961640	-0.23765911110488	-4.96112756971547
H	-6.11738348183505	-0.24312922439917	-3.95448718712527
H	-5.65921533665384	0.85114171900495	-2.66901105703263
H	-5.10508539791852	-1.85679258619664	-0.27360810337877
H	-5.71883652265385	-2.08919115855001	-2.56339559556626
H	-5.37022877728682	0.78922908730657	-0.04383698725152
H	-3.98051553877648	-0.00105312978929	0.69310106094700
H	-2.90064760214415	1.74849161519900	-0.36648547427647
H	-4.03853879470890	1.84134844009432	-1.69169917484626
H	-3.47969934147413	-3.33872978526022	-1.67480136199273
H	-0.75269728976822	-1.31628601243374	-0.15091601103458
H	-2.50795408052030	-1.85833807800665	-0.47879683709288
H	-3.40090768634983	-2.42990818850194	-3.56807448885436

10. References

The numbering of these references carries on from the numbering in the main article.

[17] D. J. Heldebrant, P. G. Jessop, C. A. Thomas, C. A. Eckert and C. L. Liotta, *J. Org. Chem*., **2005**, *70*, 5335–5338

[18] CrysAlisPro Software System, Rigaku Oxford Diffraction, **2023**.

[19] G. M. Sheldrick, *Acta Cryst*. **2015**, *A71*, 3.

[20] O. V. Dolomanov, L. J. Bourhis, R. J. Gildea, J. A. K. Howard, H. Puschmann, *Appl. Cryst*. **2009**, *42*, 339.

[21] L. J. Bourhis, O. V. Dolomanov, R. J. Gildea, J. A. K. Howard, H. Puschmann, *Acta Cryst. A*, **2015**, *A71*, 59.

[22] F. Neese, *WIREs Comput. Mol. Sci.* **2017**, e1327.

[23] F. Neese, *J. Comp. Chem.* **2003**, *24*, 1740.

[24] S. Grimme, S. Ehrlich, L. Goerigk, *J. Comp. Chem*. **2011**, *32*, 1456.

[25] a) F. Weingrad, R. Aldrichs, *Phys. Chem. Chem. Phys*. **2005**, *7*, 3297; b) A. Schaefer, H. Horn, R. Aldrichs, *J. Chem. Phys*. **1992**, *97*, 2571.

[26] B. Helmich-Paris, B. de Souza, F. Neese, R. Izsák, *J. Chem. Phys*., **2021**, *155*, 104109.

[27] N. Mardirossian, M. Head-Gordon, *J. Chem. Phys*., **2016**, *144*, 214110.

[28] C.-K. Skylaris, L. Gagliardi, N. C. Handy, A. GIoannou, S. Spencer, A. Willetts, *J. of Mol. Str. (Theochem)* **2000**, *501*, 229.

[29] A. V. Marenich, C. J. Cramer, D. G. Truhlar, *J. Phys. Chem. B*. **2009**, *113*, 6378.

[30] a) J. Tao, J. P. Perdew, V. N. Staroverov, G. E. Scuseria, *Phys. Rev. Lett.* **2003**, *91*, 146401; b) V. N. Staroverov, G. E. Scuseria, J. Tao, J. P. Perdew, *J. Chem. Phys*. **2003**, *119*, 12129.

[31] a) F. Jensen, *J. Chem. Theory Comput*. **2015**, *11*, 132; b) G. L. Stoychev, A. A. Auer, F. Neese, *J. Chem. Theory Comput*. **2017**, *13*, 554.

[32] G. L. Stoychev, A. A. Auer, F. Neese, *J. Chem. Theory Comput*. **2018**, *14*, 4756.

[33] J. D. Rolfes, F. Neese, D. A. Pantazis, *J. Comput. Chem*. **2020**, *41*, 1842.

[34] T. Lu, F. Chen, *J. Comput. Chem*. **2012**, *33*, 580.